Materials Today Electronics 7 (2024) 100081

Contents lists available at ScienceDirect

Materials Today Electronics

journal homepage: www.elsevier.com/locate/mtelec

Full Length Article

Compositional engineering of magnetic anisotropy in $Cr_2Si_xGe_{2-x}Te_6$

Ti Xie [a,1], Shanchuan Liang [a,1], Samuel Deitemyer [b,1], Qinqin Wang [a,1], Tong Zhou [c], Igor Žutić [c], Xixiang Zhang [d], Dongsheng Yuan [e,*], Xiang Zhang [f,*], Cheng Gong [a,*]

[a] Department of Electrical and Computer Engineering and Quantum Technology Center, University of Maryland, College Park, Maryland 20742, United States
[b] Department of Physics, University of Maryland, College Park, Maryland 20742, United States
[c] Department of Physics, University at Buffalo, State University of New York, Buffalo, New York 14260, United States
[d] Physical Sciences and Engineering Division (PSE), King Abdullah University of Science and Technology (KAUST), Thuwal 23955-6900, Saudi Arabia
[e] National Institute for Materials Science (NIMS), 1-1 Namiki, Tsukuba, Ibaraki 305-0044, Japan
[f] Faculty of Science and Faculty of Engineering, The University of Hong Kong, Hong Kong, China

ARTICLE INFO

Keywords:
2D van der Waals magnets
Magnetic anisotropy
Compositional engineering

ABSTRACT

Magnetic van der Waals (vdW) materials are highly sensitive to their chemical compositions and atomic structures, which presents rich opportunities for synthetic control of vdW ferromagnets. Here, we synthesized the quaternary alloys $Cr_2Si_xGe_{2-x}Te_6$ using the flux method and discovered that the Ge:Si source ratio should be designed deliberately higher than the expected in resultant crystals due to the stronger affinity of Si than Ge to be involved in $Cr_2Si_xGe_{2-x}Te_6$ reactions. Temperature-dependent magnetization and magnetic hysteresis measurements revealed that as the Si content increases, the Curie temperature decreases while the out-of-plane anisotropy increases monotonically. When x increases from 0 to 2 in $Cr_2Si_xGe_{2-x}Te_6$, the out-of-plane saturation fields remain approximately unchanged at ~0.2 T, while the in-plane saturation fields increase monotonically from 0.5 T to 1.2 T. The distinct behaviors between out-of-plane and in-plane saturation fields arise from the different mechanisms underpinning the two fields – the out-of-plane saturation field is determined by the competition of exchange interaction, magnetic anisotropy, and dipolar interaction, whereas the in-plane saturation field by magnetic anisotropy. Our compositional engineering provides a fundamental understanding of the layered magnetic materials and insightful guidance for the future design of vdW magnets.

The discovery of long-range magnetic order in two-dimensional (2D) van der Waals (vdW) crystals [1–5] has demonstrated that easy-axis magnetic anisotropy can resist thermal fluctuations by opening a spin-wave excitation gap, thereby allowing for the existence of long-range magnetic order with finite Curie temperatures (T_C) in 2D systems [6–9]. Given that 2D materials exhibit a wide range of electronic structures and properties, ranging from wide bandgap [10], zero-gap [11], to correlated states [12], the intrinsic ferromagnetism in these layered electronic systems could expand the material platforms for devices with enhanced functionalities [13–16]. Furthermore, the weak vdW interlayer forces allow the exfoliation and restacking of monolayers into arbitrary heterostructures with controllable magnetic properties [17–19]. Among the vdW magnetic materials, magnetic insulators (MI) are a unique class of materials differing from metallic magnets, and particularly, they could allow the propagation of spin wave without involving charge current and Joule heating, promising energy-efficient spintronic devices [20–22]. By interfacing with other electronic and topological materials (e.g., Bi_2Te_3) [23,24], vdW MI such as $Cr_2Ge_2Te_6$ (CGT) can imprint the magnets' spin-polarized wavefunction into the neighboring materials, enabling the anomalous Hall effect, without shunting the charge current.

Chromium chalcogenides, such as CGT and $Cr_2Si_2Te_6$ (CST), as prototypical vdW MIs, exhibit a wide range of intriguing physical properties, including tunable magnetism [25–27] and complex magnetic domains [28]. A unique property of CGT stems from its small easy-axis anisotropy, rendering 2D CGT as a close-to-ideal 2D Heisenberg model [1,29]. Understanding and controlling the anisotropy of CGT and its isostructural compounds could have a significant impact on both the fundamental physics of 2D Heisenberg magnets and the development of emerging 2D spintronic devices [6].

In this work, we study the compositional engineering of $Cr_2Si_xGe_{2-x}Te_6$ and find that both T_C and saturation fields are tunable by

* Corresponding authors.
E-mail addresses: yuan.dongsheng@nims.go.jp (D. Yuan), president@hku.hk (X. Zhang), gongc@umd.edu (C. Gong).
[1] These authors contributed equally.

https://doi.org/10.1016/j.mtelec.2023.100081
Received 29 April 2023; Received in revised form 17 November 2023; Accepted 17 November 2023
Available online 22 November 2023

varying the Si/Ge composition, indicating the fine chemical tunability of the exchange interaction and magnetic anisotropy. Notably, we observe that the out-of-plane saturation fields in all $Cr_2Si_xGe_{2-x}Te_6$ compounds remain almost constant at ~0.2 T, while the in-plane saturation fields increase monotonically from 0.5 T to 1.2 T as x varies from 0 to 2. The distinct behaviors between the out-of-plane and in-plane saturation fields are attributed to the different mechanisms underlying the two fields. Specifically, the out-of-plane saturation field is determined by the competition of exchange interaction, magnetic anisotropy, and dipolar interaction, while the in-plane saturation field is primarily governed by magnetic anisotropy alone. This capability to continuously engineer crystals with tunable structures and compositions opens possibilities for new materials with tailored magnetic properties and creates a platform that can be used to study fundamental magnetic parameters such as exchange interaction, magnetocrystalline anisotropy, and dipole interactions of vdW magnets.

CGT and CST are MIs with Curie temperatures of 66 K and 33 K for bulk crystals, respectively [1,30]. Both materials are isostructural compounds belonging to space-group R-3 with rhombohedral symmetry. In general, these are 1T AB_2 layered crystals composed of stacked layers of a pair of two chromium (Cr) atoms and one tetrel dimer (Si for CST and Ge for CGT) in an octahedral plane, sandwiched between planes of tellurium (Te) atoms, as shown in Fig. 1(a). Figure 1(b) illustrates the top-view crystal structures of CST, CGT, and the hybrid $Cr_2Si_xGe_{2-x}Te_6$ alloys. The specific choice between Si (CST) or Ge (CGT) will result in a different degree of trigonal distortion of the crystal lattice, which will affect the geometry of the system and thus the electrostatic environment. Since the origin of magnetocrystalline anisotropy is rooted in the crystal field, it is reasonable to expect the magnetic anisotropy of $Cr_2Si_xGe_{2-x}Te_6$ to vary as a function of x.

$Cr_2Si_xGe_{2-x}Te_6$ presents a unique opportunity to explore the magnetic properties with adjustable crystallographic parameters due to the similarity of crystal structures between CGT and CST [1,30]. Here we synthesized the quaternary alloys $Cr_2Si_xGe_{2-x}Te_6$ with various Ge:Si ratios by employing the flux method [23]. We designed $Cr_2Si_xGe_{2-x}Te_6$ with various x values ($x = 2$, 1.2, 0.48, 0.28, and 0), where $x = 2$ and $x = 0$ correspond to crystals of $Cr_2Si_2Te_6$ and $Cr_2Ge_2Te_6$, respectively (The detailed chemical synthesis process is introduced in the Supplemental Material). We found that to achieve the desired Ge:Si ratios, the quantity of Ge source should be purposely more than the amount expected in the final synthesized crystals because Si has a stronger affinity in $Cr_2Si_{x-}Ge_{2-x}Te_6$ synthesis reactions than Ge. The stoichiometry and phase purity of each crystal were determined from energy-dispersive X-ray spectroscopy (EDX) and the well-defined layers on the crystal edge from the scanning electron microscopy (SEM) image (Fig. S1 and Fig. S2 in Supplemental Material). We next performed vibrating-sample magnetometry to examine the magnetic properties of the synthesized bulk crystals.

We conducted magnetization measurements on $Cr_2Si_xGe_{2-x}Te_6$ crystals under a 0.1 T out-of-plane magnetic field during the temperature increasing process. Fig. 2(a) shows the normalized magnetization of $Cr_2Si_xGe_{2-x}Te_6$ with varying Si content (x) at temperatures ranging from 4 K to 120 K. We observed a monotonic decrease in the ferromagnetic transition temperature (T_C) with increasing Si content, revealing that for all synthesized $Cr_2Si_xGe_{2-x}Te_6$ alloys, the T_C values lie between the T_C of CST and that of CGT, as summarized in Fig. 2(b). The critical temperatures for $Cr_2Si_xGe_{2-x}Te_6$ crystals with x values of 2, 1.2, 0.48, 0.28, and 0 were identified at 33 K, 43 K, 51 K, 58 K, and 66 K, respectively, the two boundaries of which are consistent with the previously reported T_C values of bulk CGT and CST crystals [1,30]. The magnetization values of $Cr_2Si_xGe_{2-x}Te_6$ are ~2.7 μ_B/Cr (Fig. S3 in Supplemental Material). Since the magnetization of $Cr_2Si_xGe_{2-x}Te_6$ arises from the magnetic moment of Cr, changing x will not result in an obvious change in the magnetization of $Cr_2Si_xGe_{2-x}Te_6$. In 3D systems, exchange interaction (J) is a key factor in determining the T_C value. We found that T_C decreases as the Si content increases, suggesting that J decreases with Si content, which implicates possible approaches for continuous tuning of exchange interaction in vdW magnets.

The normalized field-dependent magnetizations of $Cr_2Si_xGe_{2-x}Te_6$ compounds are summarized in Fig. 3(a) with magnetic fields externally applied perpendicular to the crystallographic plane. All measurements in Fig. 3 are conducted at 4 K. The magnetizations saturate around 0.2 T when the external magnetic fields are applied perpendicular to the ab-plane (i.e., $B_\perp$), and remain virtually constant for all values of x. In contrast, when external fields are applied parallel to the ab-plane (i.e., $B_\parallel$), saturation fields vary from 0.5 T to 1.2 T for different values of Si

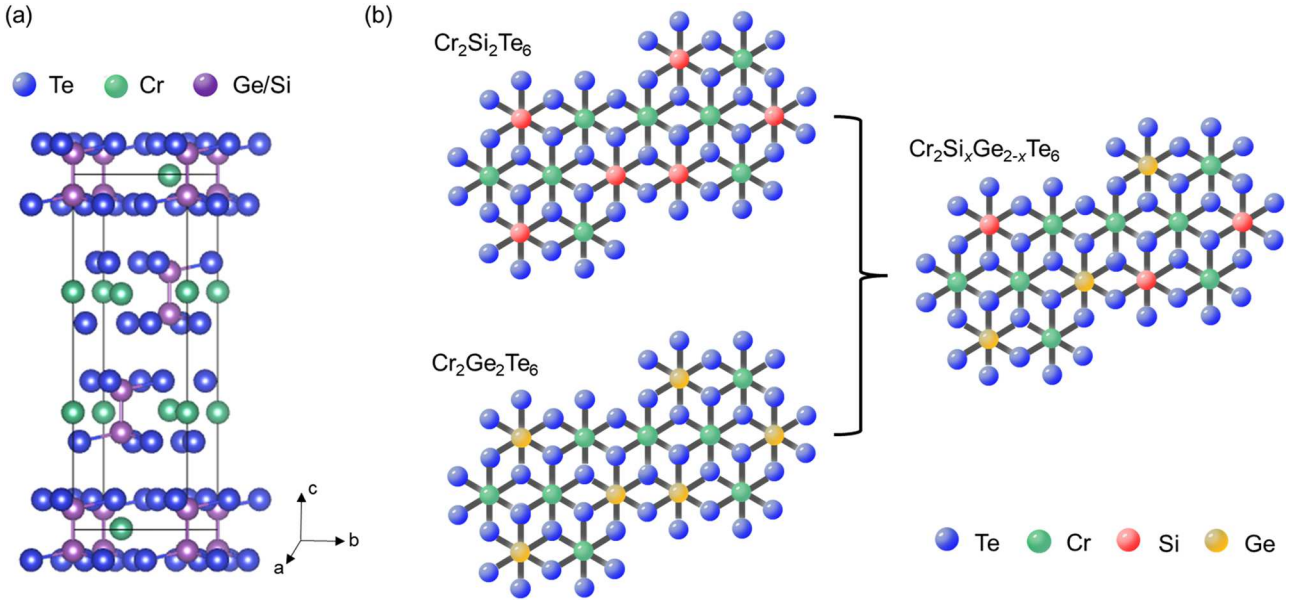

Fig. 1. Schematic crystal structures of $Cr_2Si_xGe_{2-x}Te_6$. (a) Side view of $Cr_2(Si/Ge)_2Te_6$ unit cell. The side view illustrates the slightly distorted octahedral plane composed of two Cr atoms and a Si-Si or Ge-Ge dimer, sandwiched between planes of Te atoms. (b) Top-view conceptual illustration of the atomic structures of CST, CGT, and a representative $Cr_2Si_xGe_{2-x}Te_6$ alloy. Each Cr atom is surrounded by six Te atoms, which are further surrounded by three Si-Si or Ge-Ge dimers in equivalent positions around the central Cr atom.

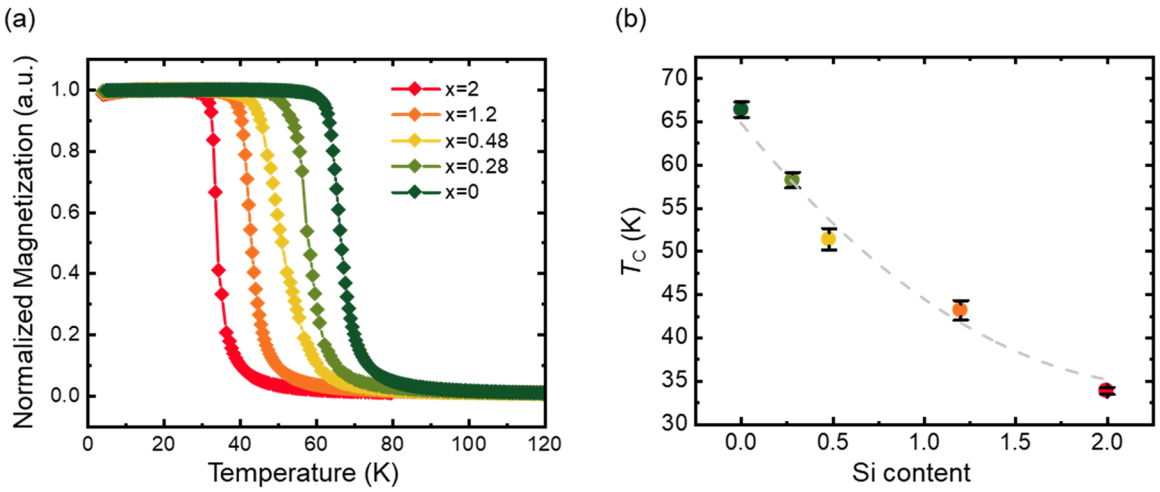

Fig. 2. Temperature-dependent magnetization and the extracted Curie temperatures of $Cr_2Si_xGe_{2-x}Te_6$ for various values of x. (a) Normalized magnetization versus temperature for $Cr_2Si_2Te_6$ (red), $Cr_2Si_{1.2}Ge_{0.8}Te_6$ (orange), $Cr_2Si_{0.48}Ge_{1.52}Te_6$ (yellow), $Cr_2Si_{0.28}Ge_{1.72}Te_6$ (light green), and $Cr_2Ge_2Te_6$ (dark green). (b) Measured T_C of each synthesized crystal versus Si content, x. The dashed line represents a second-order polynomial fit. Error bars arise from the uncertainty in T_C identification based on the raw data of temperature dependent magnetization.

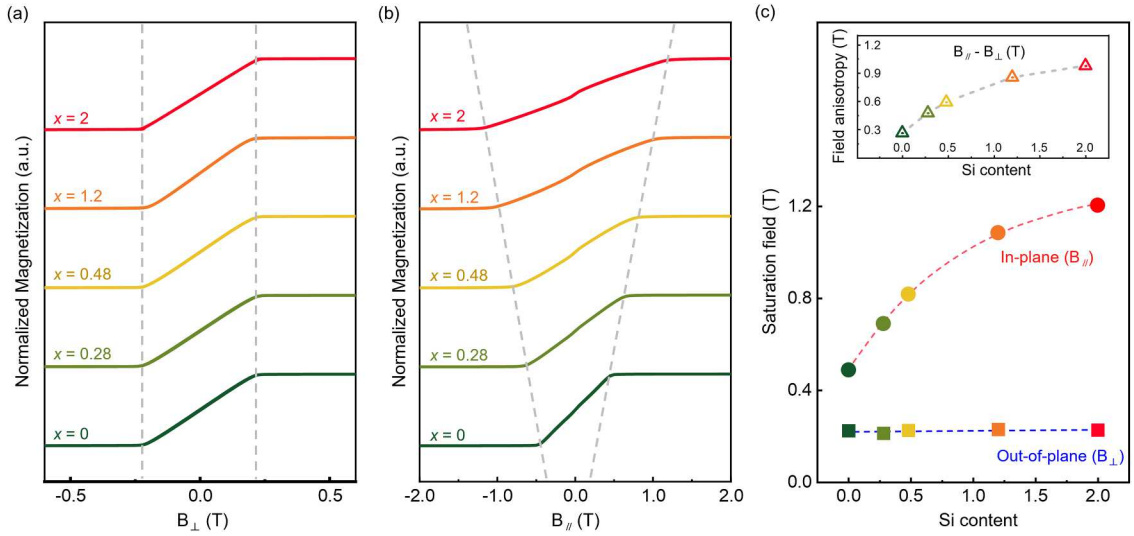

Fig. 3. Magnetic hysteresis measurements for $Cr_2Si_xGe_{2-x}Te_6$ compounds when the magnetic field is externally applied (a) perpendicular and (b) parallel to the crystallographic ab-plane for different values of Si contents, expressed by x. Dashed lines serve as references to the eye. When the external field is perpendicular to the ab-plane (a), the saturation field remains constant at 0.2 T for all the studied compounds. For fields applied parallel to the ab-plane (b), the saturation field increases from 0.5 T for $x = 0$ to 1.2 T for $x = 2$. (c) Summary of the Si content dependent saturation fields of $Cr_2Si_xGe_{2-x}Te_6$ for external fields applied perpendicular ($B_\perp$) and parallel ($B_\parallel$) to the crystallographic ab-plane. Inset shows the field anisotropy versus Si content and the gray dashed line represents an exponential fit. Field anisotropy is defined as the absolute difference between saturation fields for $B_\parallel$ and $B_\perp$ for each synthesized crystal. Blue and red dashed lines represent linear and exponentially asymptotic fits, respectively. Error bars represent the standard deviation of the read-out saturation fields and are smaller than the plotted points.

contents (Fig. 3(b)). It is worth noting that the lowest saturation field for $B_\parallel$ is 0.5 T with $x = 0$, which is larger than the nearly constant 0.2 T saturation field for $B_\perp$, indicating that the crystallographic *c*-axis is the magnetic easy-axis for all synthesized alloys.

Fig. 3(c) summarizes the saturation fields of all $Cr_2Si_xGe_{2-x}Te_6$ compounds for external fields applied out-of-plane (blue, linear fit) and in-plane (red, exponential asymptotic fit). Note that out-of-plane saturation fields are approximately unchanged at ~0.2 T, while the in-plane saturation fields increase monotonically from 0.5 T to 1.2 T as *x* increases from 0 to 2 in $Cr_2Si_xGe_{2-x}Te_6$. The contrast in the compositional dependence of the saturation fields along the in-plane and out-of-plane directions arises from the different mechanisms underpinning the two fields, which will be discussed later. Here we define the field anisotropy of all synthesized alloys as the difference between saturation fields for $B_\parallel$ and $B_\perp$. We find that the field anisotropy of CGT and CST are 0.3 T and 1.0 T, respectively, which agrees well with previously reported results [31,32]. Furthermore, the field anisotropy of each alloy falls in between these two values, following a continuous increase of easy-axis magnetocrystalline anisotropy with increasing Si content (Fig. 3(c) inset).

Here we provide an insight into the phenomenon described in Fig. 3 (c) – namely, that the out-of-plane saturation field remains constant for all compounds, while the in-plane saturation field grows monotonically with increasing Si content in the compounds. For out-of-plane magnetic fields larger than the saturation field, all spins are aligned towards the orientations of the externally applied out-of-plane fields, as illustrated in the regions I and V in Fig. 4(a). Nonetheless, a decrease in the magnitude of the applied out-of-plane external field results in a reduction in magnetization due to the formation of multiple domains, given that both

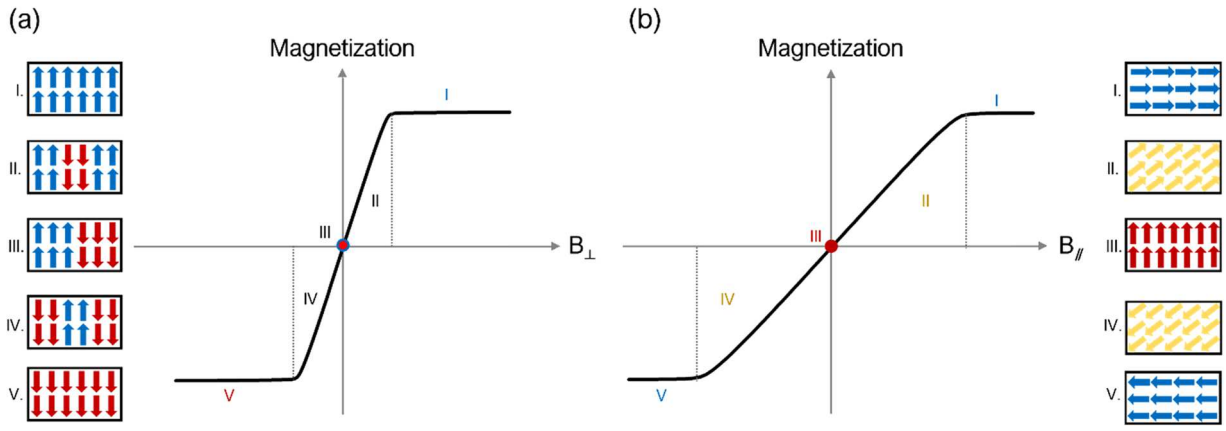

Fig. 4. Schematics of fundamental mechanisms for how the magnetization of $Cr_2Si_xGe_{2-x}Te_6$ varies with the magnetic fields applied along different directions. (a) When an external field is applied perpendicular to the crystal basal plane, a relatively small field suffices to saturate the magnetization (a-I). Magnetization decreases with the decreasing magnetic field, due to the formation of multiple magnetic domains (a-II, a-III). Then, magnetization increases as spins start to align with the increasing opposite magnetic field (a-IV) until magnetization saturates (a-V). (b) If an external field is applied parallel to the crystal basal plane, a relatively large field is necessary to align all spins (b-I). As the field decreases in magnitude, spins start to bend towards the magnetic easy-axis, decreasing the measured in-plane magnetization (b-II). At zero field, all spins align along the easy-axis, therefore zeroing the in-plane magnetization (b-III). As the field increases in magnitude in the opposite direction, spins will be forced to bend toward the field direction. This will increase the in-plane magnetization (b-IV) until the magnetization is saturated along the direction of the external magnetic field (b-V).

CGT and CST exhibit easy-axis ferromagnetism. Under these circumstances, the competition among exchange interactions (J), magnetic anisotropy (A), and dipolar interaction (D) determines the out-of-plane saturation field. Specifically, J and A tend to preserve the single-domain state, while D tends to promote multi-domains. For $Cr_2Si_xGe_{2-x}Te_6$, it can be regarded as a combination of CGT and CST. Our results reveal that the exchange interaction of CGT (J_{CGT}) is larger than the exchange interaction of CST (J_{CST}), as reflected by their T_C (i.e., higher T_C represents larger J); the anisotropy of CGT (A_{CGT}) is smaller than CST (A_{CST}); the dipolar interaction of $Cr_2Si_xGe_{2-x}Te_6$ remains nearly the same for all values of x, which is due to the small difference (~1%) in lattice constant between CGT and CST [33,34] and the same magnetic ion. Consequently, CGT, CST, and all intermediate alloys exhibit similar amounts of magnetization. Therefore, if the larger exchange interaction in CGT approximately counteracts the smaller magnetic anisotropy in CST, then CGT and CST will have the same energy increase (exchange interaction and anisotropy) and the same energy decrease (dipolar interaction) during the formation of multiple domains. As a result, it is possible that the out-of-plane saturation fields are approximately unchanged when x increases from 0 to 2 in $Cr_2Si_xGe_{2-x}Te_6$.

When the external field is applied parallel to the crystallographic plane, the field-dependent magnetization progresses differently since the external field forces the spins to align against anisotropy. In this case, the field necessary to overcome the out-of-plane anisotropy will align all spins along an in-plane direction (regions I and V in Fig. 4(b)). Here, the presence of a strong external field maintains spins along the in-plane orientation, and when this field is reduced below the saturation field, magnetization decreases as the spins begin to rotate towards the easy-axis [35]. At the origin (Fig. 4(b)-III), all spins point out-of-plane, yielding zero in-plane magnetization. As the external field increases, now in the opposite direction, all spins are forced to bend again (Fig. 4 (b)-IV), increasing the magnetization until the system eventually reaches another saturation point when all spins are aligned with the field, as illustrated by the region V in Fig. 4(b). It is evident that the in-plane saturation field is determined by magnetic anisotropy, and therefore the in-plane saturation fields of $Cr_2Si_xGe_{2-x}Te_6$ change as x changes, considering the different anisotropies of CGT and CST. This spin-rotation process, when the external magnetic field is applied along the hard axis, fundamentally differs from the multi-domain formation process when the external magnetic field is applied along the easy-axis.

In summary, we present a facile alloying scheme to finely tune the chemical composition in a quaternary $Cr_2Si_xGe_{2-x}Te_6$ system. We found that the T_C decreases and the easy-axis anisotropy increases monotonically with increasing Si content. Interestingly, the out-of-plane saturation fields are approximately unchanged for all compounds studied, while the in-plane saturation fields increase monotonically from 0.5 T to 1.2 T as x increases from 0 to 2 in $Cr_2Si_xGe_{2-x}Te_6$. The observed distinct behaviors between out-of-plane and in-plane saturation fields stem from the different mechanisms underpinning the two fields. Our work provides fundamental understanding and valuable guidance for the future design of vdW magnets.

Supplemental materials

See the supplemental material for the crystal synthesis details and the detailed SEM, EDX, and temperature-dependent magnetization characterization of the synthesized alloys.

CRediT authorship contribution statement

Ti Xie: Formal analysis, Visualization, Writing – original draft, Writing – review & editing. **Shanchuan Liang:** Visualization, Writing – original draft, Writing – review & editing. **Samuel Deitemyer:** Writing – original draft, Writing – review & editing. **Qinqin Wang:** Visualization, Writing – original draft, Writing – review & editing. **Tong Zhou:** Formal analysis. **Igor Žutić:** Formal analysis, Supervision. **Xixiang Zhang:** Supervision. **Dongsheng Yuan:** Data curation, Formal analysis, Investigation, Methodology, Visualization. **Xiang Zhang:** Supervision, Project administration. **Cheng Gong:** Conceptualization, Formal analysis, Funding acquisition, Supervision, Visualization, Writing – original draft, Writing – review & editing, Project administration.

Declaration of Competing Interest

The authors declare no competing interests.

Data availability

The data that support the findings of this study are available from the corresponding authors upon reasonable request.

Acknowledgments

C.G. acknowledges the grant support from Air Force Office of Scientific Research under Award No. FA9550–22–1-0349, Naval Air Warfare Center Aircraft Division under Award No. N00421–22–1-0001, Army Research Laboratory under Cooperative Agreement No. W911NF-19–2-0181, and National Science Foundation under Award No. CMMI-2233592 and No. 49100423C0011. T.X. gives thanks to V.Z.C. for her early engagement in this research.

Supplementary materials

Supplementary material associated with this article can be found, in the online version, at doi:10.1016/j.mtelec.2023.100081.

References

[1] C. Gong, L. Li, Z. Li, H. Ji, A. Stern, Y. Xia, T. Cao, W. Bao, C. Wang, Y. Wang, Z. Q. Qiu, R.J. Cava, S.G. Louie, J. Xia, X. Zhang, Discovery of intrinsic ferromagnetism in two-dimensional van der Waals crystals, Nature 546 (2017) 265–269, https://doi.org/10.1038/nature22060.

[2] B. Huang, G. Clark, E. Navarro-Moratalla, D.R. Klein, R. Cheng, K.L. Seyler, D. Zhong, E. Schmidgall, M.A. McGuire, D.H. Cobden, W. Yao, D. Xiao, P. Jarillo-Herrero, X. Xu, Layer-dependent ferromagnetism in a van der Waals crystal down to the monolayer limit, Nature 546 (2017) 270–273, https://doi.org/10.1038/nature22391.

[3] Z. Fei, B. Huang, P. Malinowski, W. Wang, T. Song, J. Sanchez, W. Yao, D. Xiao, X. Zhu, A.F. May, W. Wu, D.H. Cobden, J.H. Chu, X. Xu, Two-dimensional itinerant ferromagnetism in atomically thin Fe_3GeTe_2, Nat. Mater. 17 (2018) 778–782, https://doi.org/10.1038/s41563-018-0149-7.

[4] A.F. May, D. Ovchinnikov, Q. Zheng, R. Hermann, S. Calder, B. Huang, Z. Fei, Y. Liu, X. Xu, M.A. McGuire, Ferromagnetism near room temperature in the cleavable van der Waals crystal Fe_5GeTe_2, ACS Nano 13 (2019) 4436–4442, https://doi.org/10.1021/acsnano.8b09660.

[5] M. Moaied, J. Lee, J. Hong, A 2D ferromagnetic semiconductor Cr-trihalide and its Janus structures, Phys. Chem. Chem. Phys. 20 (2018) 21755–21763, https://doi.org/10.1039/C8CP03489C.

[6] C. Gong, X. Zhang, Two-dimensional magnetic crystals and emergent heterostructure devices, Science 363 (2019) eaav4450, https://doi.org/10.1126/science.aav4450.

[7] M. Gibertini, M. Koperski, A. Morpurgo, K. Novoselov, Magnetic 2D materials and heterostructures, Nat. Nanotechnol. 14 (2019) 408–419, https://doi.org/10.1038/s41565-019-0438-6.

[8] K.S. Burch, D. Mandrus, J.G. Park, Magnetism in two-dimensional van der Waals materials, Nature 563 (2018) 47–52, https://doi.org/10.1038/s41586-018-0631-z.

[9] X. Jiang, Q. Liu, J. Xing, N. Liu, Y. Guo, Z. Liu, J. Zhao, Recent progress on 2D magnets: fundamental mechanism, structural design, and modification, Appl. Phys. Rev. 8 (2021), 031305, https://doi.org/10.1063/5.0039979.

[10] G. Cassabois, P. Valvin, B. Gil, Hexagonal boron nitride is an indirect bandgap semiconductor, Nat. Photon. 10 (2016) 262–266, https://doi.org/10.1038/nphoton.2015.277.

[11] A.K. Geim, K.S. Novoselov, The rise of graphene, Nat. Mater. 6 (2007) 183–191, https://doi.org/10.1038/nmat1849.

[12] B. Radisavljevic, A. Kis, Mobility engineering and a metal–insulator transition in monolayer MoS_2, Nat. Mater. 12 (2013) 815–820, https://doi.org/10.1038/nmat3687.

[13] M. Liu, J. Leveillee, S. Lu, J. Yu, H. Kim, C. Tian, Y. Shi, K. Lai, C. Zhang, F. Giustino, C.K. Shih, Monolayer 1T-$NbSe_2$ as a 2D-correlated magnetic insulator, Sci. Adv. 7 (2021) eabi6339, https://doi.org/10.1126/sciadv.abi6339.

[14] J.X. Zhu, M. Janoschek, D.S. Chaves, J.C. Cezar, T. Durakiewicz, F. Ronning, Y. Sassa, M. Mansson, B.L. Scott, N. Wakeham, E.D. Bauer, J.D. Thompson, Electronic correlation and magnetism in the ferromagnetic metal Fe_3GeTe_2, Phys. Rev. B 93 (2016), 144404, https://doi.org/10.1103/PhysRevB.93.144404.

[15] T. Song, Q.C. Sun, E. Anderson, C. Wang, J. Qian, T. Taniguchi, K. Watanabe, M. A. McGuire, R. Stöhr, D. Xiao, T. Cao, J. Wrachtrup, X. Xu, Direct visualization of magnetic domains and moiré magnetism in twisted 2D magnets, Science 374 (2021) 1140–1144, https://doi.org/10.1126/science.abj7478.

[16] B. Huang, G. Clark, D.R. Klein, D. MacNeill, E. Navarro-Moratalla, K.L. Seyler, N. Wilson, M.A. McGuire, D.H. Cobden, D. Xiao, W. Yao, P. Jarillo-Herrero, X. Xu, Electrical control of 2D magnetism in bilayer CrI_3, Nat. Nanotechnol. 13 (2018) 544–548, https://doi.org/10.1038/s41565-018-0121-3.

[17] R. Zhu, W. Zhang, W. Shen, P. Wong, Q. Wang, Q. Liang, Z. Tian, Y. Zhai, C.W. Qiu, A.T.S. Wee, Exchange bias in van der Waals $CrCl_3/Fe_3GeTe_2$ heterostructures, Nano Lett 20 (2020) 5030–5035.

[18] J. Shang, X. Tang, X. Tan, A. Du, T. Liao, S.C. Smith, Y. Gu, C. Li, L. Kou, Stacking-dependent interlayer magnetic coupling in 2D $CrI_3/CrGeTe_3$ nanostructures for spintronics, ACS Appl. Nano Mater. 3 (2020) 1282–1288, https://doi.org/10.1021/acsanm.9b02055.

[19] S. Albarakati, W.Q. Xie, C. Tan, G. Zheng, M. Algarni, J. Li, J. Partridge, M.J. S. Spencer, L. Farrar, Y. Xiong, M. Tian, X. Wang, Y.J. Zhao, L. Wang, Electric control of exchange bias effect in $FePS_3$–Fe_5GeTe_2 van der Waals heterostructures, Nano Lett. 22 (2022) 6166–6172, https://doi.org/10.1021/acs.nanolett.2c01370.

[20] Y. Kajiwara, K. Harii, S. Takahashi, J. Ohe, K. Uchida, M. Mizuguchi, H. Umezawa, H. Kawai, K. Ando, K. Takanashi, S. Maekawa, E. Saitoh, Transmission of electrical signals by spin-wave interconversion in a magnetic insulator, Nature 464 (2010) 262–266, https://doi.org/10.1038/nature08876.

[21] L.J. Cornelissen, J. Liu, R.A. Duine, J. Ben Youssef, B.J. van Wees, Long-distance transport of magnon spin information in a magnetic insulator at room temperature, Nat. Phys. 11 (2015) 1022–1026, https://doi.org/10.1038/nphys3465.

[22] A.E. Allcca, X.C. Pan, I. Miotkowski, K. Tanigaki, Y.P. Chen, Gate-tunable anomalous Hall effect in stacked van der Waals ferromagnetic insulator−topological insulator heterostructures, Nano Lett 22 (2022) 8130–8136, https://doi.org/10.1021/acs.nanolett.2c02571.

[23] H. Ji, R.A. Stokes, L.D. Alegria, E.C. Blomberg, M.A. Tanatar, A. Reijnders, L. M. Schoop, T. Liang, R. Prozorov, K.S. Burch, N.P. Ong, J.R. Petta, R.J. Cava, A ferromagnetic insulating substrate for the epitaxial growth of topological insulators, J. Appl. Phys. 114 (2013), 114907, https://doi.org/10.1063/1.4822092.

[24] L.D. Alegria, H. Ji, N. Yao, J.J. Clarke, R.J. Cava, J. .R. Petta, Large anomalous Hall effect in ferromagnetic insulator-topological insulator heterostructures, Appl. Phys. Lett. 105 (2014), 053512, https://doi.org/10.1063/1.4892353.

[25] S. Liang, T. Xie, N.A. Blumenschein, T. Zhou, T. Ersevim, Z. Song, J. Liang, M. A. Susner, B.S. Conner, S.J. Gong, J.P. Wang, M. Ouyang, I. Žutić, A.L. Friedman, X. Zhang, C. Gong, Small-voltage multiferroic control of two-dimensional magnetic insulators, Nat. Electron. 6 (2023) 199–205, https://doi.org/10.1038/s41928-023-00931-1.

[26] Z. Wang, T. Zhang, M. Ding, B. Dong, Y. Li, M. Chen, X. Li, J. Huang, H. Wang, X. Zhao, Y. Li, D. Li, C. Jia, L. Sun, H. Guo, Y. Ye, D. Sun, Y. Chen, T. Yang, J. Zhang, S. Ono, Z. Han, Z. Zhang, Electric-field control of magnetism in a few-layered van der Waals ferromagnetic semiconductor, Nat. Nanotechnol. 13 (2018) 554–559, https://doi.org/10.1038/s41565-018-0186-z.

[27] I.A. Verzhbitskiy, H. Kurebayashi, H. Cheng, J. Zhou, S. Khan, Y. .P. Feng, G. Eda, Controlling the magnetic anisotropy in $Cr_2Ge_2Te_6$ by electrostatic gating, Nat. Electron. 3 (2020) 460–465, https://doi.org/10.1038/s41928-020-0427-7.

[28] S. Wu, L. Wang, B. Gao, Y. Wang, Y.S. Oh, S.W. Cheong, J. Hong, X. Wang, The direct observation of ferromagnetic domain of single crystal $CrSiTe_3$, AIP Adv 8 (2018), 055016, https://doi.org/10.1063/1.5024576.

[29] N.D. Mermin, H. Wagner, Absence of ferromagnetism or antiferromagnetism in one-or two-dimensional isotropic Heisenberg models, Phys. Rev. Lett. 17 (1966) 1133–1136, https://doi.org/10.1103/PhysRevLett.17.1133.

[30] V. Carteaux, G. Ouvrard, J.C. Grenier, Y. Laligant, Magnetic structure of the new layered ferromagnetic chromium hexatellurosilicate $Cr_2Si_2Te_6$, J. Magn. Magn. Mater. 94 (1991) 127–133, https://doi.org/10.1016/0304-8853(91)90121-P.

[31] X. Zhang, Y. Zhao, Q. Song, S. Jia, J. Shi, W. Han, Magnetic anisotropy of the single-crystalline ferromagnetic insulator $Cr_2Ge_2Te_6$, Jpn. J. Appl. Phys. 55 (2016), 033001, https://doi.org/10.7567/JJAP.55.033001.

[32] Y. Liu, C. Petrovic, Anisotropic magnetic entropy change in $Cr_2X_2Te_6$ (X= Si and Ge), Phys. Rev. Mater. 3 (2019), 014001, https://doi.org/10.1103/PhysRevMaterials.3.014001.

[33] V. Carteaux, D. Brunet, G. Ouvrad, G. Andre, Crystallographic, magnetic and electronic structures of a new layered ferromagnetic compound $Cr_2Ge_2Te_6$, J. Phys. Condens. Matter 7 (1995) 69–87, https://doi.org/10.1088/0953-8984/7/1/008.

[34] G. Ouvrard, E. Sandre, R. Brec, Synthesis and crystal structure of a new layered phase: the chromium hexatellurosilicate $Cr_2Si_2Te_6$, J. Solid State Chem. 73 (1988) 27–32, https://doi.org/10.1016/0022-4596(88)90049-7.

[35] C. Boix-Constant, S. Mañas-Valero, A.M. Ruiz, A. Rybakov, K.A. Konieczny, S. Pillet, J.J. Baldoví, E. Coronado, Probing the spin dimensionality in single-layer CrSBr van der Waals heterostructures by magneto-transport measurements, Adv. Mater. 34 (2022), 2204940, https://doi.org/10.1002/adma.202204940.